USGS Award No. 03HQGR0040

# EVALUATION OF SITE EFFECTS DURING THE 1999 CHI-CHI EARTHQUAKE AND ITS AFTERSHOCKS

**Ellen M. Rathje, Ph.D.**
University of Texas at Austin
ECJ 9.227, C1792
Austin, TX 78712
Tel: 512-471-4929
Fax: 512-471-6548
e.rathje@mail.utexas.edu
http://www.ce.utexas.edu/dept/area/geotech/GeotechnicalEngr.htm

**NEHRP Element:** II
**Key Words:** Site Effects, Ground Amplification, Building Codes

*Research supported by the U.S. Geological Survey (USGS), Department of the Interior, under USGS award number (03HQGR0040). The views and conclusions contained in this document are those of the authors and should not be interpreted as necessarily representing the official policies, either expressed or implied, of the U.S. Government*

## ABSTRACT

The objective of this research is a study of the ground motions from the 1999 ($M_w$ = 7.6) Chi-Chi, Taiwan earthquake and its aftershocks considering the effect of soil conditions on ground shaking. Peak ground acceleration and acceleration response spectra were studied for the mainshock and aftershocks. Event-specific attenuation relationships for peak ground acceleration and spectral acceleration at various periods and different site conditions were developed for the Chi-Chi mainshock and six aftershocks ($M_w$ range 5.3 to 6.3). Site amplification factors ($S_{a,SOIL}/S_{a,ROCK}$) were derived from the regression results These amplification factors were compared with those from current building codes. Results indicate that the observed amplification at stiffer sites (Site Classes C and D) during the mainshock was similar to the values used in the International Building Code (IBC 2003). The amplification observed during the aftershocks generally was within +/- 20% of the amplification observed during the mainshock. However, for softer sites (Site Class E), the amplification observed during the mainshock was smaller than currently incorporated in IBC (2003) and the amplification varied significantly among the aftershocks. Additionally, long period amplification was significant at Site Class E sites and was potentially caused by surface wave generation at these soft sites.

## NON-TECHNICAL SUMMARY

Soil conditions can significantly affect the amplitude and frequency of ground shaking during earthquakes. Recordings of ground shaking during previous earthquakes provide a wealth of knowledge regarding the amplification of ground shaking due to soil conditions and can be compared with the amplification predicted by numerical simulation and incorporated in current building codes. This study investigated the amplification indicated by strong motion recordings from the 1999 ($M_w$ = 7.6) Chi-Chi, Taiwan earthquake and its aftershocks. The amplification at stiffer sites was similar to that incorporated in building codes, but the softer sites showed amplification significantly different than previously expected. The observations from the Chi-Chi earthquakes and its aftershocks can be used to re-evaluate the amplification factors incorporated in current building codes.

## INTRODUCTION

The objective of this research is a study of the ground motions from the 1999 ($M_w$ = 7.6) Chi-Chi, Taiwan earthquake and its aftershocks considering the effect of soil conditions on ground shaking. Peak ground acceleration and acceleration response spectra were studied for the mainshock and aftershocks. A site classification study was performed at 26 strong motion stations in Taiwan where new shear wave velocity data were available. These new classifications were compared with previous studies to ensure the accuracy of the site classifications at these strong motion stations. Event-specific attenuation relationships for peak ground acceleration and spectral acceleration at various periods and different site conditions were developed for the Chi-Chi mainshock and six aftershocks ($M_w$ range 5.3 to 6.3). Site amplification factors ($S_{a,SOIL}/S_{a,ROCK}$) were derived from the regression results from the event-specific attenuation relationships. These amplification factors were compared with those from current building codes.

## SITE CLASSIFICATION

The site classification systems considered in this study are the International Building Code (IBC 2003) system (International Code Council 2003), the Simplified Geotechnical Site (SGS) classification system (Rodriguez-Marek et al. 2001), and the Geomatrix (GM) system (Geomatrix 1993). The UBC system is based on the average shear wave velocity over the top 30 m ($\overline{V}_s$). The UBC site classes include hard rock ($S_A$, $\overline{V}_s$ > 1500 m/s), rock ($S_B$, $\overline{V}_s$ = 760-1500 m/s), very dense soil and soft rock ($S_C$, $\overline{V}_s$ = 360-760 m/s), stiff soil ($S_D$, $\overline{V}_s$ = 180-360 m/s), and soft soil ($S_E$, $\overline{V}_s$ < 180 m/s). A site also may be classified as soft soil if more than 3 m of soft clay is present. The SGS system is based on soil type and depth, which makes the soil classes related to site period. The SGS classes include rock (B, soil depth < 6 m), soft rock and shallow soil (C, soil depth < 60 m), deep stiff soil (D, soil depth > 60 m), and soft soil (E, soft soil thickness >3 m). Finally, the GM system separates rock (A), shallow soil (B, soil depth < 20 m), and deep soil (C, soil depth > 20 m in a narrow canyon; D, soil depth > 20 m in a wide canyon). Soft soil (E) is defined based on a shear wave velocity less than 150 m/s.

Initial UBC site classifications for the strong motion stations in Taiwan were based on geologic and geomorphologic data (Lee et al., 2001). At this time, these site classifications are considered the best estimates of the site conditions at the strong motion stations in Taiwan. Bray (2003) used this site class information to develop SGS classes for each site. Unfortunately, many stations could not be conclusively classified due to inconsistencies in the geologic and borehole data. Therefore, Stokoe et al. (2003) measured shear wave velocities at 26 critical strong motion stations in Taiwan using the spectral-analysis-of-surface-waves (SASW) method and used this information to define site classes based on the UBC site classification system. In this study, site classifications were reconsidered at the 26 critical strong motion stations characterized by Stokoe et al (2003). These sites were classified in terms of the UBC, SGS, and GM site classification systems. The re-evaluated site classes are listed in Table 1, along with the classes defined in the previous studies.

**Table 1.** Comparison of the site classes for strong motion stations.

| General Description | | | Bray (2003) | Stokoe et al. (2003) | | This Study | | Final SGS Site Classification | Comments[4] |
|---|---|---|---|---|---|---|---|---|---|
| No | Site Location | Station | SGS Class | Average Vs (m/s) | UBC (1997) | GM Geomatrix (1993) | SGS (2001) | | |
| 1 | Lin-Chong Elem. School | CHY-024 | D | 427 | $S_C$ | D | C - D[2] | D | |
| 2 | Ton-Lo Elem. School | TCU-039 | C | 552 | $S_C$ | B | C | C | Rock at 18 m |
| 3 | Cheou-Shio Elem. School | TCU-049 (OYO)[3] | D | 454 | $S_C$ | D | C | C[1] | Rock at 32 m |
| 4 | Wu-Fon Elem. School | TCU-065 (OYO)[3] | D | 244 | $S_D$ | D | C | C[1] | Rock at ~ 55 - 60 m |
| 5 | Si-Kon Elem. School | TCU-068 | D | 506 | $S_C$ | D | C - D[2] | D | |
| 6 | Suan-Don Elem. School | TCU-071 | C | 588 | $S_C$ | B | C | C | Rock at 9 m |
| 7 | Kuo-Sing Elem. School | TCU-072 (OYO)[3] | D | 411 | $S_C$ | B | C | C[1] | Rock at ~ 15 - 27 m |
| 8 | Nan-Kon Elem. School | TCU-074 | D | 418 | $S_C$ | D | C - D[2] | D | |
| 9 | Chiou-Tun Elem. School | TCU-075 (OYO)[3] | D | 451 | $S_C$ | B | C | C[1] | Rock at 19 m |
| 10 | Nan-To Elem. School | TCU-076 (OYO)[3] | D | 533 | $S_C$ | B-D | C | C[1] | Rock at ~ 18 - 26 m |
| 11 | Shai-Li Elem. School | TCU-078 | D | 469 | $S_C$ | B | C | C[1] | Rock at 18 m |
| 12 | Tor-Se Elem. School | TCU-079 | D | 424 | $S_C$ | D | C | C[1] | Rock at ~ 30 m |
| 13 | Fon-Ton High School | TCU-102 (OYO)[3] | D | 539 | $S_C$ | B | C | C[1] | Rock at ~ 15 - 20 m |
| 14 | Nai-Pu Elem. School | TCU-103 | D | 628 | $S_C$ | B | C | C[1] | Rock at 18 m |
| 15 | Yuan-Lin Elem. School | TCU-110 (OYO)[3] | E | 213 | $S_D$ | E | E | E | Vs ~150 m/s in top 15 m |
| 16 | Sin-Hua Elem. School | TCU-113 | E | 237 | $S_D$ | E | E | E | Vs ~150 m/s in top 5 m |
| 17 | Si-Hu Elem. School | TCU-115 | E | 229 | $S_D$ | E | E | E | Vs ~150 m/s in top 9 m |
| 18 | Ten-Chong High School | TCU-116 | E | 381 | $S_C$ | D | C - D[2] | D[1] | Minimum Vs ~ 200 m/s |
| 19 | Ton-Ang Elem. School | TCU-120 | C | 415 | $S_C$ | D | C - D[2] | C | |
| 20 | A-Sua Elem. School | TCU-122 | D | 475 | $S_C$ | D | C | C[1] | Rock at 22 m |
| 21 | Cheng-Jung Elem. School | TCU-128 | C | 524 | $S_C$ | B | C | C | Rock at 14 m |
| 22 | Sin-Jai Elem. School | TCU-129 | D | 664 | $S_C$ | B | C | C[1] | Rock at 18 m |
| 23 | Kung-Chung Elem. School | TCU-052 | D | 393 | $S_C$ | D | C - D[2] | D | |
| 24 | Sin-San Elem. School | TCU-054 (OYO)[3] | D | 488 | $S_C$ | D | C | C[1] | Rock at ~ 20 - 29 m |
| 25 | Tai -Chung Weather Station | TCU-082 (OYO)[3] | D | 399 | $S_C$ | D | C - D[2] | D | |
| 26 | Chi-Nan University | TCU-148 (OYO)[3] | No data | 424 | $S_C$ | D | C | C[1] | Rock at ~20 - 27 m |

1- The final BRM class changed from previous study (only changed classification if evidence conclusive regarding site class).
2- Soil profile did not extend to a depth of 60 m to allow conclusive assignment to SGS-C or SGS-D.
3- OYO log profile at larger depth taken into account with SASW profile at shallow depth.
4- Rock defined by $V_s > 760$ m/s.

When examining Table 1, there are some differences between the final assigned SGS site classes and previous site classification studies. Based on the current study, thirteen SGS-D sites (deep stiff soil) were changed to SGS-C sites (shallow soil) because rock was encountered in the Vs profiles at depths less than 60 m. Additionally, one SGS-E site (soft soil) was changed to SGS-D because no soft soil was encountered at the site.

## EVENT-SPECIFIC ATTENUATION RELATIONSHIPS

### Chi-Chi Mainshock

The Chi-Chi mainshock generated a significant number of strong motion recordings within 130 km from the fault. Nonlinear regression techniques were used to develop event-specific attenuation relationships for peak ground acceleration (PGA) and spectral acceleration ($S_a$) at various periods. The event-specific attenuation relationships were developed for each SGS site class (SGS-B, -C, -D, -E). The distribution of these data versus distance for each site category is given in Figure 1.

The form of the event-specific attenuation relationship used in this study is:

$$\ln Y = c_1 + c_2 \,.\, \ln\left(\sqrt{R^2 + c_3{}^2}\right) + \sigma \qquad (1)$$

where Y is the ground motion parameter (PGA and $S_a$ at various periods) in units of gravity, R is the closest distance to the fault rupture plane in km, $c_1$, $c_2$ and $c_3$ are regression coefficients, and $\sigma$ is an error term that was evaluated by using the ordinary least square method. Equation 1 was fit to PGA and $S_a$ at periods of 0.3, 1.0, and 2.0 seconds using the strong motion data from distances between 0 and 130 km. The regression was performed separately for each site class (i.e., SGS-B, -C, -D and -E).

In the regression analyses, the $c_3$ parameter was calculated for each ground motion parameter using the data from all site categories. This value was then constrained to this value for each site class and the regression performed again for each site class to obtain coefficients $c_1$ and $c_2$.

Initially, three different studies were considered using the strong motion data. These studies considered the motions from (a) 0 to 130 km, (b) 0 to 100 km, and (c) 1 to 100 km. These distance ranges were considered because the strong motion data are not evenly distributed with distance for some site classes (Figure 1). The number of recordings for each site class within different distance bins is shown in Table 2. Table 2 indicates that almost no data fall in the distance range of 0-1 km for each of the site classes. Additionally, there are limited data for B and C sites in the distance range between 100 and 130 km. There is a significant amount of strong motion data for all site classes in the distance range of 10 to 100 km and for site classes C and D in the distance range 1 to 10 km. The initial regression was performed only with the data in the distance range of 1 to 100 km, which allows the important C and D data at distances less than 10 km to be included. The data at distances less than 1 km and greater than 100 km were excluded so as not to bias the results. The regression coefficients and standard error terms for the initial event-specific attenuation relationships that were developed using the strong motion data from between 1 and 100 km are shown in Table 3.

**Table 2.** The distribution of strong motion data with respect to distance and site class for the Chi-Chi mainshock.

| km | B-Site | C-Site | D-Site | E-Site | Total |
|---|---|---|---|---|---|
| **0-1** | 0 | 0 | 3 | 0 | 3 |
| **1-10** | 0 | 6 | 19 | 0 | 25 |
| **10-100** | 25 | 48 | 136 | 50 | 259 |
| **100-130** | 11 | 6 | 20 | 39 | 76 |

**Table 3.** Initial regression coefficients and error terms for event-specific attenuation relationships for Chi-Chi mainshock.

| 1-100 km | PGA | | | | Sa (T=0.3) | | | | Sa (T=1.0) | | | | Sa (T=2.0) | | | |
|---|---|---|---|---|---|---|---|---|---|---|---|---|---|---|---|---|
| Site Class | SGS-B | SGS-C | SGS-D | SGS-E | SGS-B | SGS-C | SGS-D | SGS-E | SGS-B | SGS-C | SGS-D | SGS-E | SGS-B | SGS-C | SGS-D | SGS-E |
| $c_1$ | -0.752 | 0.389 | 0.641 | -0.778 | 0.995 | 1.313 | 2.036 | 0.022 | -0.049 | 1.329 | 0.874 | -0.298 | -1.045 | 0.533 | -0.047 | 0.129 |
| $c_2$ | -0.547 | -0.738 | -0.786 | -0.459 | -0.749 | -0.734 | -0.923 | -0.442 | -0.652 | -0.895 | -0.668 | -0.405 | -0.599 | -0.866 | -0.606 | -0.583 |
| $c_3$ | 8.889 | 8.889 | 8.889 | 8.889 | 12.439 | 12.439 | 12.439 | 12.439 | 11.108 | 11.108 | 11.108 | 11.108 | 9.111 | 9.111 | 9.111 | 9.111 |
| $\sigma$ | 0.412 | 0.592 | 0.466 | 0.288 | 0.532 | 0.628 | 0.519 | 0.329 | 0.428 | 0.559 | 0.474 | 0.370 | 0.438 | 0.619 | 0.505 | 0.373 |

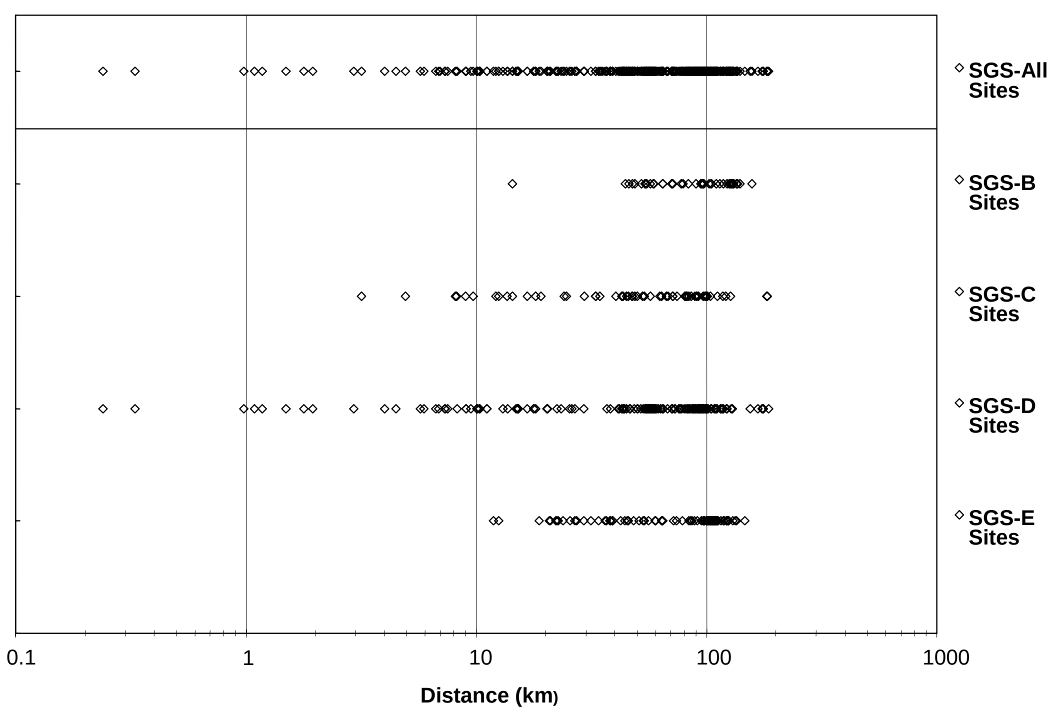


**Figure 1.** Distribution of Chi-Chi mainshock data according to site category and distance.

Table 2 and Figure 1 indicate that the majority of the strong motion data was recorded at distances greater than 10 km. In fact, there are no rock (site class SGS-B) recordings for distances less than 10 km and only one rock recording between 10 and 40 km (Figure 1). Because one aim of this study was to evaluate site amplification with respect to rock motions, the lack of rock data at distances less than 40 km presents a problem. If these regression results for rock sites are used as the basis for site response factors (i.e., $S_{a,SOIL}/S_{a,ROCK}$), unrealistic site response factors may result. The initial PGA regression results for SGS-B are shown in Figure 2, along with the recorded rock data. The curve is well constrained at distances between 40 and 100 km because of the large amount of data in this distance range. However, there is less confidence in the curve at distances less than 40 km because there is only one data point in this distance range.

When developing site response factors using the initial SGS-B regression as a base, unusually large amplification was predicted for soil sites at distances less than 40 km. Because of the unusual result and the uncertainty in the SGS-B regression at smaller distances, further constraints were imposed on the SGS-B regression. The regression parameter $c_2$ was developed using SGS-B and SGS-C data, which are more evenly distributed across distances (Figure 1). Finally, the parameter $c_1$ was developed using the SGS-B data only. The constrained SGS-B regression results are presented in Figure 3, along with the initial SGS-B regression results. The constrained regression is similar to the initial regression at large distances, but is higher than the initial regression at shorter distances. The final regression coefficients and standard error terms, developed by constraining $c_2$ for SGS-B sites, are shown in Table 4. The final regression results together with the initial regression results are plotted in Figure 4 for PGA and $S_a$ at periods of 0.3, 1.0 and 2.0 seconds.

The PGA relationships (Figure 4a) indicate that PGA amplitudes at soil sites (SGS-C, -D, and -E) are similar for distances greater than about 50 km. At shorter distances, SGS-C and -D sites have the largest PGA values. The regression results for T=0.3 s (Figure 4b) also show similar values of $S_a$ for SGS-C, -D, and -E sites at longer distances. At shorter distances, the deep soil sites (SGS-D) show the largest $S_a$. The regression results for T=1.0 s (Figure 4c) indicate the largest values of $S_a$ for SGS-D and -E site at large distances, and for SGS-D and -C at shorter distances. The regression results for T=2.0 s (Figure 4d) indicate that values of $S_a$ are largest for soft soil sites (SGS-E) across all distances. This result occurs because amplification of long periods at soft soil sites is considerably greater than for the other site classes.

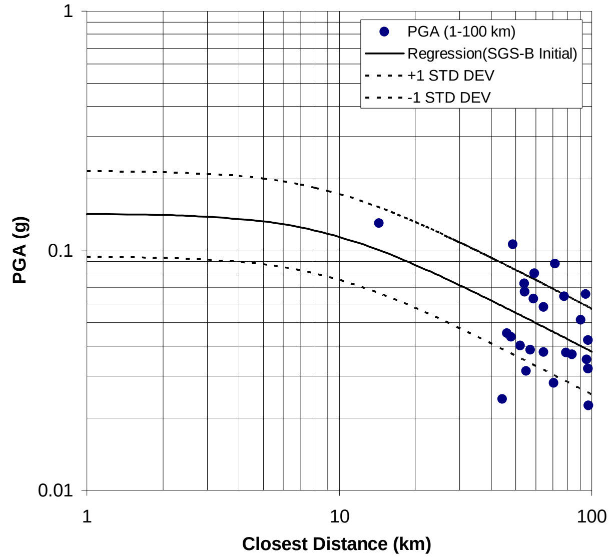


**Figure 2.** Initial SGS-B regression results for rock sites (mainshock).

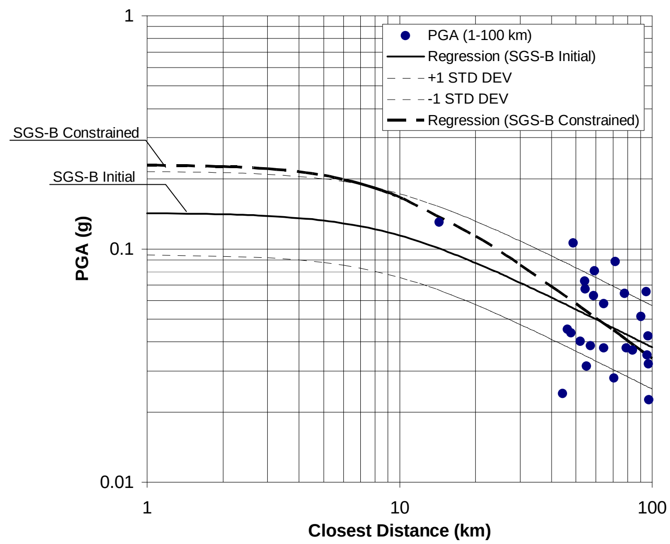


**Figure 3.** The constrained and the original SGS-B regression results for rock sites (mainshock).

**Table 4.** Final regression coefficients and error terms for event-specific attenuation relationships for Chi-Chi mainshock.

| 1-100 km | PGA | | | | Sa (T=0.3) | | | | Sa (T=1.0) | | | | Sa (T=2.0) | | | |
|---|---|---|---|---|---|---|---|---|---|---|---|---|---|---|---|---|
| Site Class | SGS-B | SGS-C | SGS-D | SGS-E | SGS-B | SGS-C | SGS-D | SGS-E | SGS-B | SGS-C | SGS-D | SGS-E | SGS-B | SGS-C | SGS-D | SGS-E |
| $c_1$ | 0.258 | 0.389 | 0.641 | -0.778 | 1.300 | 1.313 | 2.036 | 0.022 | 1.189 | 1.329 | 0.874 | -0.298 | 0.356 | 0.533 | -0.047 | 0.129 |
| $c_2$ | -0.790 | -0.738 | -0.786 | -0.459 | -0.882 | -0.734 | -0.923 | -0.442 | -0.949 | -0.895 | -0.668 | -0.405 | -0.936 | -0.866 | -0.606 | -0.583 |
| $c_3$ | 8.889 | 8.889 | 8.889 | 8.889 | 12.439 | 12.439 | 12.439 | 12.439 | 11.108 | 11.108 | 11.108 | 11.108 | 9.111 | 9.111 | 9.111 | 9.111 |
| $\sigma$ | 0.413 | 0.592 | 0.466 | 0.288 | 0.521 | 0.628 | 0.519 | 0.329 | 0.433 | 0.559 | 0.474 | 0.370 | 0.447 | 0.619 | 0.505 | 0.373 |

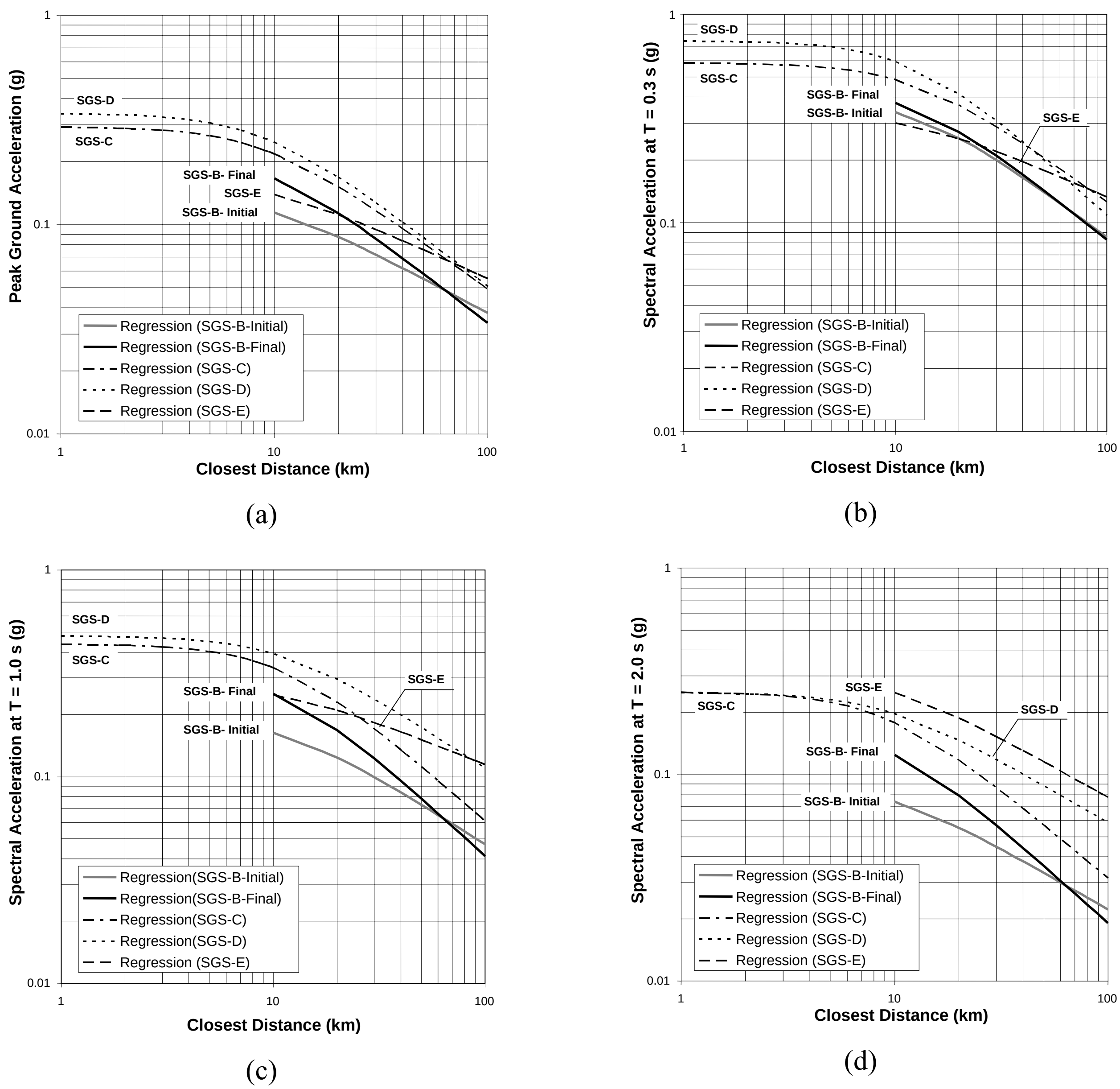


**Figure 4.** Results from Chi-Chi mainshock regression analyses for (a) PGA and $S_a$ at periods of (b) 0.3, (c) 1.0, and (d) 2.0 seconds from.

## Chi-Chi Aftershocks

Event-specific attenuation relationships were developed for six Chi-Chi aftershocks, as listed in Table 5. Data from distances between 1 an 100 km were used in the regression. Although each event was recorded by well over 100 strong motion stations, the distribution of the recordings across site classes and distance was not always adequate. In particular, the number and distribution of SGS-B sites presented a challenge for most of the events. The $M_w$ 5.8 event had the most even coverage of SGS-B sites, although the minimum distance recorded was about 30 km. The other events had difficulties related to the number of SGS-B recordings, the minimum distance recorded by SGS-B sites (sometimes as large as 70 to 80 km), or the uneven distance distribution of SGS-B data. For some of these events, several constraints were applied to the regression to get reasonable amplification results.

**Table 5.** Chi-Chi aftershocks analyzed and the number of recordings for each site class.

| Magnitude | Date | No. B Sites | No. C Sites | No. D Sites | No. E Sites |
|---|---|---|---|---|---|
| 5.8 | 9/20/99 17:57 | 16[1] (30[2]) | 31 (48) | 104 (141) | 43 (70) |
| 6.2-a | 9/20/99 18:03 | 10 (14) | 40 (46) | 102 (127) | 37 (50) |
| 5.3 | 9/20/99 19:40 | 7 (7) | 21 (25) | 59 (68) | 41 (43) |
| 6.2-b | 9/20/99 21:46 | 13 (15) | 36 (37) | 108 (120) | 50 (66) |
| 6.2-c | 9/22/99 00:14 | 12 (34) | 31 (48) | 101 (156) | 36 (81) |
| 6.3 | 9/25/99 23:52 | 12 (22) | 29 (48) | 93 (147) | 31 (75) |

[1] Number of sites used in analysis (distances less than 100 km)
[2] Total number of sites

Each Chi-Chi aftershock was analyzed using a procedure similar to that used for the mainshock. The coefficient $c_3$ was determined based on all data from all site classes for that event. To best constrain the SGS-B regression, which often had limited data, the coefficient $c_2$ was developed using the combined SGS-B and SGS-C data, and then coefficient $c_1$ was developed using only SGS-B data. The resulting regression coefficients for each site class and each event are shown in Table 6.

**Table 6.** Regression coefficients and error terms for event-specific attenuation relationships for Chi-Chi aftershocks.

**9/20/99 - 17:57 - Mw=5.8**

| 1-100 km | PGA | | | | Sa (T=0.3) | | | | Sa (T=1.0) | | | | Sa (T=2.0) | | | |
|---|---|---|---|---|---|---|---|---|---|---|---|---|---|---|---|---|
| | SGS-B | SGS-C | SGS-D | SGS-E | SGS-B | SGS-C | SGS-D | SGS-E | SGS-B | SGS-C | SGS-D | SGS-E | SGS-B | SGS-C | SGS-D | SGS-E |
| $c_1$ | -2.200 | -1.945 | -1.193 | -1.755 | -1.671 | -1.381 | -0.474 | -0.570 | -1.555 | -1.150 | -1.350 | -0.665 | -3.192 | -2.701 | -3.355 | -0.595 |
| $c_2$ | -0.515 | -0.515 | -0.638 | -0.477 | -0.426 | -0.426 | -0.577 | -0.550 | -0.773 | -0.773 | -0.615 | -0.784 | -0.815 | -0.815 | -0.507 | -1.190 |
| $c_3$ | 5.000 | | | | 5.000 | | | | 5.000 | | | | 5.000 | | | |
| σ | 0.637 | 0.656 | 0.686 | 0.486 | 0.670 | 0.599 | 0.673 | 0.523 | 0.784 | 0.923 | 0.840 | 0.674 | 0.805 | 1.183 | 0.982 | 0.896 |

**9/20/99 - 18:03 - Mw=6.2**

| 1-100 km | PGA | | | | Sa (T=0.3) | | | | Sa (T=1.0) | | | | Sa (T=2.0) | | | |
|---|---|---|---|---|---|---|---|---|---|---|---|---|---|---|---|---|
| | SGS-B | SGS-C | SGS-D | SGS-E | SGS-B | SGS-C | SGS-D | SGS-E | SGS-B | SGS-C | SGS-D | SGS-E | SGS-B | SGS-C | SGS-D | SGS-E |
| $c_1$ | 0.654 | 1.054 | 3.406 | -0.759 | 0.735 | 1.328 | 3.677 | -0.258 | 0.078 | 0.784 | 2.591 | 1.120 | -0.377 | 0.723 | 1.753 | 0.504 |
| $c_2$ | -1.228 | -1.228 | -1.817 | -0.622 | -1.056 | -1.056 | -1.654 | -0.568 | -1.115 | -1.115 | -1.538 | -0.955 | -1.237 | -1.237 | -1.475 | -0.813 |
| $c_3$ | 5.000 | | | | 5.000 | | | | 5.000 | | | | 5.000 | | | |
| σ | 0.469 | 0.493 | 0.733 | 0.449 | 0.559 | 0.478 | 0.738 | 0.560 | 0.892 | 0.726 | 0.847 | 0.367 | 0.940 | 0.785 | 0.970 | 0.444 |

**9/20/99 - 19:40 - Mw=5.3**

| 1-100 km | PGA | | | | Sa (T=0.3) | | | | Sa (T=1.0) | | | | Sa (T=2.0) | | | |
|---|---|---|---|---|---|---|---|---|---|---|---|---|---|---|---|---|
| | SGS-B | SGS-C | SGS-D | SGS-E | SGS-B | SGS-C | SGS-D | SGS-E | SGS-B | SGS-C | SGS-D | SGS-E | SGS-B | SGS-C | SGS-D | SGS-E |
| $c_1$ | 1.961 | 1.883 | 3.636 | 1.132 | 2.851 | 3.207 | 4.651 | 0.993 | 0.276 | 0.856 | -0.320 | 5.451 | 0.272 | 1.150 | -0.018 | 4.720 |
| $c_2$ | -1.690 | -1.690 | -2.023 | -1.370 | -1.814 | -1.814 | -2.078 | -1.165 | -1.564 | -1.564 | -1.098 | -2.347 | -1.960 | -1.960 | -1.513 | -2.418 |
| $c_3$ | 5.000 | | | | 5.000 | | | | 5.000 | | | | 5.000 | | | |
| σ | 0.360 | 0.407 | 0.519 | 0.353 | 0.459 | 0.498 | 0.523 | 0.335 | 0.270 | 0.708 | 0.667 | 0.502 | 0.315 | 0.862 | 0.728 | 0.466 |

**9/20/99 - 21:46 - Mw=6.2**

| 1-100 km | PGA | | | | Sa (T=0.3) | | | | Sa (T=1.0) | | | | Sa (T=2.0) | | | |
|---|---|---|---|---|---|---|---|---|---|---|---|---|---|---|---|---|
| | SGS-B | SGS-C | SGS-D | SGS-E | SGS-B | SGS-C | SGS-D | SGS-E | SGS-B | SGS-C | SGS-D | SGS-E | SGS-B | SGS-C | SGS-D | SGS-E |
| $c_1$ | 3.602 | 3.530 | 3.218 | 0.072 | 3.609 | 3.678 | 4.026 | 0.249 | 2.698 | 3.223 | 2.593 | 1.314 | 1.861 | 2.751 | 2.308 | 0.442 |
| $c_2$ | -1.826 | -1.826 | -1.732 | -0.868 | -1.628 | -1.628 | -1.698 | -0.698 | -1.740 | -1.740 | -1.511 | -1.037 | -1.887 | -1.887 | -1.676 | -1.009 |
| $c_3$ | 5.000 | | | | 5.000 | | | | 5.000 | | | | 5.000 | | | |
| σ | 0.566 | 0.498 | 0.447 | 0.318 | 0.669 | 0.546 | 0.526 | 0.351 | 0.493 | 0.600 | 0.633 | 0.472 | 0.704 | 0.748 | 0.782 | 0.679 |

**9/22/99 - 00:14 - Mw=6.2**

| 1-100 km | PGA | | | | Sa (T=0.3) | | | | Sa (T=1.0) | | | | Sa (T=2.0) | | | |
|---|---|---|---|---|---|---|---|---|---|---|---|---|---|---|---|---|
| | SGS-B | SGS-C | SGS-D | SGS-E | SGS-B | SGS-C | SGS-D | SGS-E | SGS-B | SGS-C | SGS-D | SGS-E | SGS-B | SGS-C | SGS-D | SGS-E |
| $c_1$ | -1.520 | -0.967 | -1.385 | 0.469 | -0.471 | 0.142 | -0.591 | 0.653 | -2.552 | -1.942 | -2.378 | 0.895 | -2.769 | -1.864 | -3.814 | 0.133 |
| $c_2$ | -0.487 | -0.487 | -0.386 | -0.716 | -0.523 | -0.523 | -0.348 | -0.581 | -0.339 | -0.339 | -0.170 | -0.900 | -0.643 | -0.643 | -0.138 | -0.900 |
| $c_3$ | 5.000 | | | | 5.000 | | | | 5.000 | | | | 5.000 | | | |
| σ | 0.822 | 0.429 | 0.669 | 0.514 | 0.808 | 0.476 | 0.681 | 0.506 | 0.636 | 0.390 | 0.525 | 0.520 | 0.905 | 0.686 | 0.711 | 0.602 |

**9/25/99 23:52 Mw=6.3**

| 1-100 km | PGA | | | | Sa (T=0.3) | | | | Sa (T=1.0) | | | | Sa (T=2.0) | | | |
|---|---|---|---|---|---|---|---|---|---|---|---|---|---|---|---|---|
| | SGS-B | SGS-C | SGS-D | SGS-E | SGS-B | SGS-C | SGS-D | SGS-E | SGS-B | SGS-C | SGS-D | SGS-E | SGS-B | SGS-C | SGS-D | SGS-E |
| $c_1$ | 0.270 | 0.836 | 2.909 | 6.335 | 1.310 | 1.795 | 3.292 | 5.923 | 2.254 | 3.293 | 1.979 | -0.680 | -0.833 | 0.694 | 0.033 | -1.677 |
| $c_2$ | -0.952 | -0.952 | -1.423 | -2.067 | -0.981 | -0.981 | -1.298 | -1.792 | -1.484 | -1.484 | -1.112 | -0.421 | -1.155 | -1.155 | -0.924 | -0.361 |
| $c_3$ | 5.000 | | | | 5.000 | | | | 5.000 | | | | 5.000 | | | |
| σ | 0.567 | 0.472 | 0.631 | 0.615 | 0.577 | 0.478 | 0.660 | 0.617 | 0.457 | 0.610 | 0.646 | 0.556 | 0.626 | 0.891 | 0.978 | 0.911 |

## SITE AMPLIFICATION FACTORS

The results from the event-specific attenuation relationships were used to evaluate site amplification, or site response, factors (i.e., ratio of soil motion to rock motion). The amplification factors are a function of the soil conditions (i.e., site class) and rock motion intensity, $PGA_{rock}$. In the evaluation of the amplification ratios ($S_{a,SOIL}/S_{a,ROCK}$), the most critical point is the development of the event-specific attenuation relationships for rock (regression results for SGS-B) because this is the basis of the developed amplification ratios. As previously noted, the lack of rock data at short distances resulted in rock motions that did not give reasonable amplification factors. Therefore, the constrained regression results (Tables 4 and 6) for SGS-B were used, along with the regression results for soil sites (SGS-C, -D, and -E), to develop amplification factors for PGA and spectral acceleration at T=0.3, 1.0, and 2.0 s. The amplification factors were computed at a distance of 60 km, which represents a $PGA_{rock}$ value of 0.05 g. This distance was chosen because it is the average distance range over which Site Class B was recorded (Figure 1). It is unfortunate that the site amplification factors for this large earthquake are applicable for a very low rock intensity level. This result is caused by the lack of rock site recordings in the near-fault region and the lower than expected intensities recorded during the earthquake.

The final amplification factors for the mainshock are shown in Figure 5. For PGA, the regression indicates similar amplification (between 1.4 and 1.5) for SGS-C, -D, and -E sites (Figure 5). This is somewhat surprising, as SGS-E should display the largest amplification. Similar results were found for spectral acceleration at T=0.3 s. At longer periods (1.0 and 2.0 s), the shallow stiff sites (SGS-C) display the smallest amplification, still approximately 1.5, while the softer sites display the largest amplification, with values over 2 and 3.

The amplification factors for the best-recorded aftershock ($M_w$ = 5.8, 9/20/99 17:57) are shown in Figure 6. These amplification factors represent amplification at very low rock intensities, generally below 0.02 g. For these data, again the amplification of SGS-C averages about 1.4 for the spectral periods studied. However, in contrary to the mainshock analysis, the amplification of SGS-D and SGS-E sites deviate from the SGS-C sites at all periods. For PGA and spectral acceleration at T=0.3 s, amplification is about 1.8 for these sites. At the longer periods, amplification is well above 2.0. It is interesting that these data indicate almost the same amplification for SGS-D and SGS-E sites, as softer sites should display more amplification.

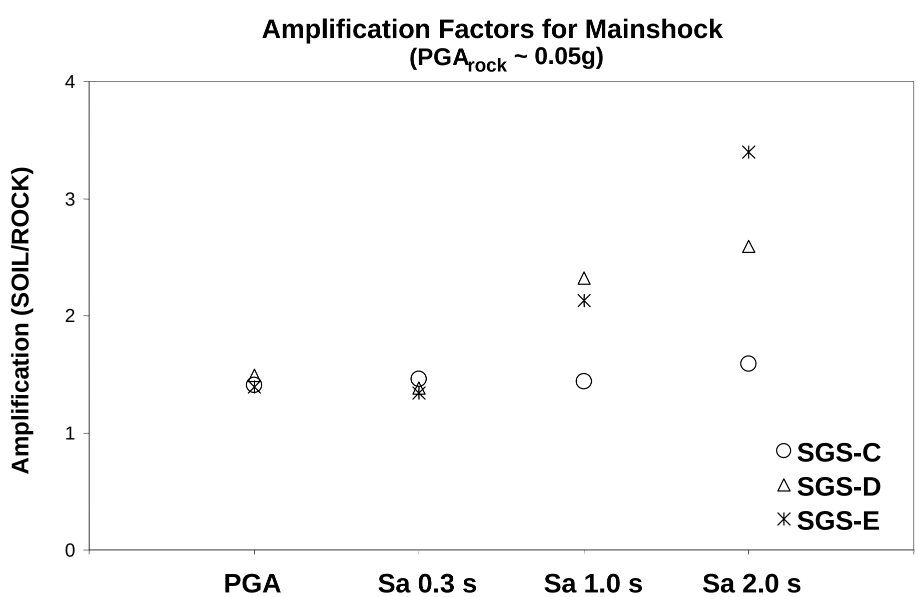


**Figure 5.** The amplification factors (SGS-C, -D and -E) for PGA and $S_a$ at periods of 0.3, 1.0, and 2.0 seconds from the Chi-Chi mainshock.

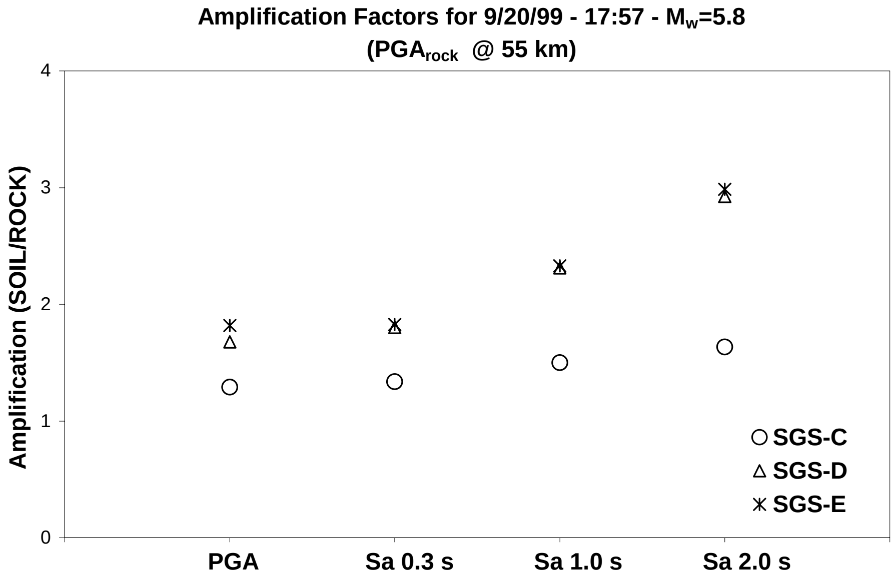


**Figure 6.** The amplification factors (SGS-C, -D and -E) for PGA and $S_a$ at periods of 0.3, 1.0, and 2.0 seconds from the $M_w$ = 5.8 (9/20/99 17:57) Chi-Chi aftershock.

The amplification factors developed for each site class and each event analyzed are listed in Table 7. These amplification factors are plotted together for each site class in Figure 7. This figure also includes the amplification factors currently recommended by IBC (2003) and those proposed by Bray and Rodriguez-Marek (B&RM 2001) for low rock intensities. It should be noted that B&RM (2001) did not develop amplification factors for soft soil sites.

For shallow stiff sites (SGS-C), the amplification factors derived from the Chi-Chi mainshock are similar to those in IBC (2003) and B&RM (2001). The Chi-Chi and B&RM (2001) factors are all around 1.5 for all spectral periods, while the IBC (2003) factors vary from 1.2 at short periods to 1.7 are long periods. The Chi-Chi aftershocks show some variability in the amplification factors (Figure 7(a)). At shorter periods, the average amplification from the aftershocks still is similar to the values proposed by others. However, at longer periods, the aftershock amplification typically is higher than the previously proposed values and those developed for the mainshock. Of all of the aftershocks, the well-recorded $M_w$ 5.8 aftershock provides amplification factors that are most consistent with the mainshock (Table 7).

**Table 7.** Amplification factors developed in this study.

| Event | Amplification Factor (SOIL/ROCK) | | | | | | | | | | | |
|---|---|---|---|---|---|---|---|---|---|---|---|---|
| | Site C / Site B | | | | Site D / Site B | | | | Site E / Site B | | | |
| | PGA | Sa (T=0.3s) | Sa (T=1.0s) | Sa (T=2.0s) | PGA | Sa (T=0.3s) | Sa (T=1.0s) | Sa (T=2.0s) | PGA | Sa (T=0.3s) | Sa (T=1.0s) | Sa (T=2.0s) |
| MainShock - $M_w$=7.6 | 1.41 | 1.46 | 1.44 | 1.59 | 1.49 | 1.38 | 2.32 | 2.59 | 1.39 | 1.34 | 2.13 | 3.40 |
| 17:57 - $M_w$=5.8 | 1.29 | 1.34 | 1.50 | 1.63 | 1.68 | 1.80 | 2.31 | 2.92 | 1.82 | 1.83 | 2.33 | 2.98 |
| 18:03 - $M_w$=6.2 | 1.49 | 1.81 | 2.03 | 3.00 | 1.28 | 1.49 | 2.04 | 3.06 | 3.20 | 2.94 | 5.60 | 14.62 |
| 19:40 - $M_w$=5.3 | 0.92 | 1.43 | 1.79 | 2.41 | 1.30 | 1.97 | 4.00 | 4.98 | 1.70 | 2.47 | 6.34 | 12.15 |
| 21:46 - $M_w$=6.2 | 0.93 | 1.07 | 1.69 | 2.44 | 1.00 | 1.14 | 2.30 | 3.71 | 1.49 | 1.57 | 4.47 | 8.84 |
| 00:14 - $M_w$=6.2 | 1.74 | 1.85 | 1.84 | 2.47 | 1.73 | 1.82 | 2.38 | 2.78 | 2.86 | 2.43 | 3.16 | 6.35 |
| 23:52 - $M_w$=6.3 | 1.76 | 1.62 | 2.83 | 4.60 | 1.89 | 1.89 | 3.69 | 6.35 | 3.77 | 3.22 | 4.87 | 12.57 |

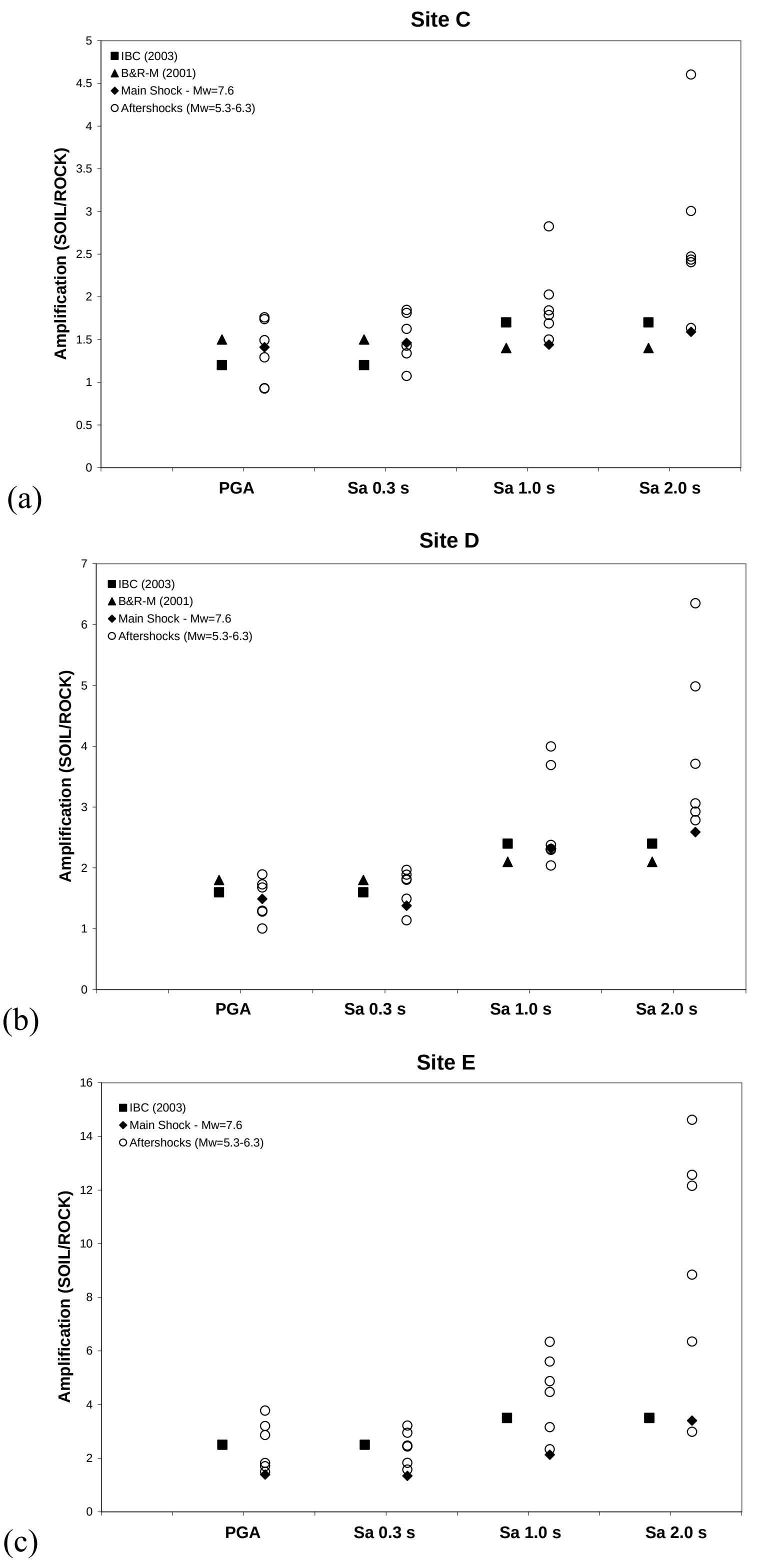


**Figure 7.** Amplification factors developed in this study for site classes SGS-C, SGS-D, and SGS-E.

Figure 7(b) shows the amplification factors developed for deep soil sites (SGS-D). The amplification factors derived from the mainshock agree well with those proposed by IBC (2003) and B&RM (2001). Again, the aftershocks show variability in the derived amplification factors. At shorter periods, the amplification factors vary from about 1.0 to 2.0. However, at longer periods (T=1.2 and 2.0 s), the variability is greater and amplification factors as large as 4.0 to 6.0 were derived.

Figure 7(c) shows the amplification factors developed for soft soil sites (SGS-E). These sites are predominantly situated on the alluvial plain on the west coast of Taiwan and were classified almost exclusively based on the surface geology, rather than in situ shear wave velocity measurements. The amplification factors derived for the mainshock for periods less than or equal to 1.0 s are about 60% of the values proposed by IBC (2003). At T=2.0 s, the Chi-Chi mainshock agrees quite well with the IBC(2003) value. Similar observations may be made of the well-recorded $M_w$ 5.8 aftershock (Table 7). However, the other aftershocks display unusually large amplification factors at long periods, particularly at T=2.0 s. Some values in excess of 10 were derived from the recorded motions. This result may be caused by surface wave motion in the soft soil records, generated at the edge of the alluvial plain. It is not clear why these surface waves did not affect the amplification factors derived for the mainshock.

## CONCLUSIONS

The large number of strong motion records obtained from the 1999 Chi-Chi earthquake and its aftershocks were processed and analyzed to evaluate the site effects observed during the earthquake. Event-specific attenuation relationships were developed for each event and each site class using data recorded at distances less than 100 km. The relationships for the various site classes were used to compute amplification factors for PGA and spectral accelerations at T = 0.3, 1.0, and 2.0 s. For shallow and deep soil sites, the amplification factors derived using the Chi-Chi mainshock data were similar to those proposed by others. For soft soil sites, the amplification factors derived for the Chi-Chi mainshock were significantly smaller than the values proposed by others. The aftershocks displayed similar amplifications factors as the mainshock at shorter periods, but these aftershocks revealed unusually large amplification factors at long periods.

## REFERENCES

Bray, J.D. (2003) Personal communication.

Geomatrix Consultants (1993) "Compilation of geotechnical data for strong-motion stations in the western United States," Report to Lawrence Livermore National Laboratory, Project No. 2256.

International Code Council (2003) *International Building Code.* International Code Council, Fall Church, VA.

Lee, C.T., Cheng, C.-T., Liao, C.-W., and Tsai, Y.-B (2001) "Site Classification of Taiwan Free-Field Strong Motions," *Bulletin of the Seismological Society of America*, Vol. 91, No.5, pp.1283-1297.

Rodriguez-Marek, A., Bray, J.D., and Abrahamson, N. (2001) "An empirically based geotechnical seismic site response procedure," *Earthquake Spectra*, 17 (1), pp.65- 88.

Stokoe, K.H., Lin, Y.H., and Rosenblad, B. (2003) "Shear Wave Velocity Profiling at Strong Motion Stations in Taiwan," Unpublished Report, University of Texas at Austin.

## PUBLICATIONS RESULTING FROM THIS WORK

Rathje, E.M, Kockar, M., and Ozbey, M.C. "Evaluation of Site Amplification during the Chi-Chi Earthquake and its Aftershocks," to be submitted to the SSA Annual Meeting, April 2005.